C. 研究結果

浜松、中国安徽省蘆江病院でとられた胃粘膜から同様の処置をおこなって DNA アダクトーム法により、付加体を検出した。とくにすでにヒト剖検例の肺組織などで検出することに成功していた、脂質過酸化に由来する7つの付加体の存在を確認し、その個体差、種々の臨床的要因、地域差などを検討した。判別分析をおこなうことによって、この7種の付加体の profile で、浜松と、蘆江病院の胃がん胃粘膜が判別できることがわかった。これらの付加体はいずれも浜松の検体で多く見られ、炎症あるいは脂質代謝関連の付加体は本邦の胃粘膜のほうによくみられることがわかった。一方、Nanosep カラムによる方法でも、陽性コントロールとしたラットの発がん系で HεdG が明瞭に同定された。

D. 考察

胃がんの頻度は、蘆江病院のある安徽省のほうが高いので、環境要因とくにアルキル付加体などの増加を期待して行ったのだが、皮肉にも炎症性付加体が本邦の胃粘膜に多いことがもっともわかりやすい結果であった。未知の付加体が多数アダクトームマップ上に現れているので、高頻度に胃がんが発生する理由に相当するような付加体をさらに検索を続けている。動物実験で知られているような有名なアルキル付加体についてはまだ検出されていない。

E. 結論

ヒト組織から DNA 付加体を検出・同定・評価することは、環境暴露要因の特定につながる有用な方法で、漠然と動物における実験発がんと同様の機構を想定してきた、ヒト発がんの原因を明らかにできる可能性がある。付加体を多種定量的に同定することもさることながら、その変異原性、細胞内での運命、修復などの生物学的課題の宝庫でもある。

F. 健康危険情報

なし

G. 研究発表

1.論文発表

1. Ella E, Sato N, Nishizawa D, Kageyama S, Yamada H, Kurabe N, Ishino K, Tao H, Tanioka F, Nozawa A, Renyin C, Shinmura K, Ikeda K, Sugimura H. Association between dopamine beta hydroxylase rs5320 polymorphism and smoking behaviour in elderly Japanese. J Hum Genet (2012), 57: 385-390.
2. Kiyose S, Igarashi H, Nagura K, Kamo T, Kawane K, Mori H, Ozawa T, Maeda M, Konno K, Hoshino H, Konno H, Ogura H, Shinmura K, Hattori N, Sugimura H. Chromogenic in situ hybridization (CISH) to detect HER2 gene amplification in breast and gastric cancer: comparison with immunohistochemistry (IHC) and fluorescence in situ hybridization (FISH). Pathol Int (2012), 62: 728-734
3. Kiyose S, Nagura K, Tao H, Igarashi H, Yamada H, Goto M, Maeda M, Kurabe N, Suzuki M, Tsuboi M, Kahyo T, Shinmura K, Hattori N, Sugimura, H. Detection of kinase amplifications in gastric cancer archives using

fluorescence in situ hybridization. Pathol Int (2012), 62: 477-484.

4. Natsume H, Shinmura K, Tao H, Igarashi H, Suzuki M, Nagura K, Goto M, Yamada H, Maeda M, Konno H, Nakamura S, Sugimura H. The CRKL gene encoding an adaptor protein is amplified, overexpressed, and a possible therapeutic target in gastric cancer. J Transl Med (2012), 10:97.
5. Sato N, Sato T, Nozawa A, Sugimura, H. Assessment Scales of Nicotine Addiction. J Addict Res Ther (2012), S1:008
6. Toyoshima M, Chida K, Suda T, Sugimura H, Sato M. Endobronchial metastasis from gastrinoma of the pancreas. Am J Respir Crit Care Med (2012), 185: 590-591.
7. Inaba K, Sakaguchi T, Kurachi K, Mori H, Tao H, Nakamura T, Takehara Y, Baba S, Maekawa M, Sugimura H, and Konno H. Hepatocellular adenoma associated with familial adenomatous polyposis coli. World J Hepatol (2013), 4: 322-326.
8. Matsuda T, Tao H, Goto M, Yamada H, Suzuki M, Wu Y, Xiao N, He Q, Guo W, Cai Z, Kurabe N, Ishino K, Matsushima Y, Shinmura K, Konno H, Maekawa M, Wang Y, Sugimura,H. Lipid Peroxidation- Induced DNA Adducts in Human Gastric Mucosa. Carcinogenesis (2013), 71:4628-4639.

2.学会発表

1. 椙村春彦、 ヒトアダクトームについて、日本分子生物学会総会、 福岡、2012 年
2. Sugimura H, Tao H, Kurabe N, Goto M, Matsushima Y, Yamada H, Shinmura K, Miyagi Y, Totsuka T, Nakagama H, Wang Y, Matsuda T. DNA Adductome, an ultimate exposome of human tissue. AACR special conference, post GWAS horizon. Hollywood, FL, USA, 2012

H. 知的財産権の出願／登録

1．なし

厚生労働科学研究費補助金（地球規模保健課題推進研究事業（国際医学協力研究事業））
分担研究報告書

新規変異原・がん原物質の検索

研究分担者　　若林 敬二　　静岡県立大学環境科学研究所　教授

研究要旨

グルコースとトリプトファンとのメイラード反応で生成する新規変異原物質 ABAQ を *gpt* delta マウスに 25 及び 50 mg/kg の用量で週 5 回、3 週間連続、経口投与すると、肝臓における点変異頻度が増加し、G→A 及び G→T 等の点突然変異が誘発されることが分かった。又、ABAQ 投与により肝臓における欠失変異頻度も、3 倍以上上昇することが分かった。更に、ABAQ はラットの尿中から検出され、その値は野生型よりも糖尿病モデル動物に於いて高値を示すことが分かった。これらの事から、糖尿病患者の生体内でも ABAQ が生成され、肝臓等の組織に変異を誘発する可能性が推測された。更に、肥満モデルマウス KK-*A*^{y} における、活性酸素種(ROS)及び脂質過酸化物(LPO)由来の DNA 付加体(8-oxodG、etheno(ε)- and heptanoneε(Hε)deoxyribonucleosides)を、LC/MS/MS を用いて解析した。その結果、 20 週齢マウス肝臓における 8-oxodG 量は、正常マウス C57BL に比べ KK-*A*^{y} で約 3 倍に増加していた。また、εdA、HεdG、HεdA、HεdC 量も、C57BL に比べ KK-*A*^{y} において 2～3 倍増加していた。これらの結果から、ROS および LPO 由来 DNA 付加体の生成が、肥満関連の発がんに寄与していることが示唆された。

A. 研究目的

肥満や糖尿病はヒトの発がんに関与することが指摘されている。しかしながら、その作用メカニズムは良くわかっていない。本研究では、グルコースとトリプトファンとのメイラード反応で生成する新規変異原物質アミノベンゾアゼピノキノリノン誘導体 5-amino-6-hydroxy-8*H*-benzo[6,7]azepino[5,4,3-*de*]quinolin-7-one (ABAQ)の遺伝毒性及び糖尿病モデル動物における in vivo 生成の有無につき解析し、ABAQ のヒト発がんへの関与の可能性について検討する。更に、肥満を呈する生体内では、活性酸素種(ROS)や脂質過酸化物(LPO)の産生が増大していることが知られている。そこで、肥満モデルマウスにおける、ROS 及び LPO 由来の DNA 付加体を解析する。本研究で得られる成果は、肥満や糖尿病とヒト発がんとの関連性を解明する上に有用なものとなる。

B. 研究方法

1. in vivo 変異原性試験

gpt delta 雄マウス(7 週齢)5 匹に ABAQ を 25 及び 50mg/kg の用量で週 5 回、3 週

間連続経口投与を行った。最終投与から 5 週目にマウスを屠殺解剖し、肝臓及び腎臓における点突然変異(gpt 変異)及び欠失変異(Spi－変異)の解析を行った。

2. ABAQ 生体内生成の解析

7～10 週齢の野生型(Wistar)、I 型(Wistar,ストレプトゾトシン投与)及び II 型糖尿病モデル(GK/Slc)雄ラット各 5 匹を代謝ケージで飼育し、24 時間分の尿を採集した。この尿サンプルを固層抽出した後に LC/MS/MS により尿中に排泄される ABAQ の量を測定した。

3. 酸化損傷に関連する DNA 付加体の解析

20 週齢の肥満モデルマウス KK-*Ay*(雌)及び対照としての正常マウス C57BL（雌)、各々、7 匹より肝臓を取り出し、常法により DNA を抽出した。DNA を Nuclease mixture 及び Alkaline phosphatase で分解し、LC/MS/MS を用いて、DNA 付加体(8-oxodG 、 etheno(ε)- and heptanoneε(Hε)deoxyribonucleosides)を、解析した。

（倫理面への配慮）

動物実験の実施に際しては、施設の動物実験倫理委員会の承認を得た後に行い、実験動物に対する動物愛護に関して十分配慮して行った。

C. 研究結果

ABAQ をマウスに経口投与すると、肝臓における点突然変異頻度が上昇し、50 mg/kg 投与群では対照群に比べ約 4 倍増加した。変異パターンを解析したところ、G→A transition 及び G→T transversion の変異を誘発することがわかった。次に、欠失変異(Spi－変異)の解析を行った。肝臓における欠失変異頻度は、対照群で $1.86\pm1.47\times10^{-6}$、ABAQ 25mg/kg 投与群で $6.17\pm2.49\times10^{-6}$、ABAQ 50mg/kg 投与群で $6.81\pm2.57\times10^{-6}$ であった。ABAQ 投与により肝臓における欠失変異頻度は明らかに増加し、25mg/kg ,50mg/kg 投与群で対照群に比べ 3 倍以上上昇した。一方、腎臓における点突然変異、及び欠失変異頻度の上昇は認められなかった。

また、ABAQ はラットの尿中から検出され、その値は野生型で 27.2±9.0 ng/24h urine、I 型糖尿病モデルで 551.1±360.8 ng/24h urine、II 型糖尿病モデルで 188.4±103.7 ng/24h urine であり、野生型よりも糖尿病モデル動物において高値を示すことがわかった。これらのことから、糖尿病患者の生体内でも ABAQ が生成され、肝臓などの組織に変異を誘発する可能性が推測された。

次に、肥満モデルマウス KK-*Ay*(雌)における、ROS および LPO 由来の DNA 付加体 (8-oxodG 、 etheno(ε)- and heptanoneε(Hε)deoxyribonucleosides)を、LC/MS/MS を用いて解析した。その結果、20 週齢マウス肝臓における 8-oxodG 量は、正常マウス C57BL に比べ KK-*Ay*で約 3 倍に増加していることがわかった。(C57BL vs KK-*Ay*: 1.36 vs 4.55 adducts/10^6 nucleotides)。また、εdA、HεdG、HεdA、HεdC 量も、C57BL に比べ KK-*Ay*において 2～3 倍増加していることが明らかとなった。(C57BL vs KK-*Ay*: 29.7、19.7、ND、ND vs 87.9 、 36.1 、 4.20 、 8.60 adducts/10^9 nucleotides)。これらの結果から、ROS および LPO 由来 DNA 付加体の生成が、肥満

関連の発がんに寄与していることが示唆された。

D. 考察

ABAQ は、*S. typhimurium* 及び CHL/IU 細胞に対して、変異原性を示すことが明らかにされている。又、ICR マウスを用いたコメットアッセイに於いて DNA 損傷作用を示すことも報告されている。更に、本研究において、ABAQ を *gpt* delta マウスに経口投与すると、肝臓において点変異頻度が上昇し、G→A 及び G→T 等の点突然変異が誘発されることが分かった。又、ABAQ 投与により肝臓における欠失変異頻度も、3 倍以上上昇することが分かった。更にこれらの、*in vitro, in vivo* における ABAQ の遺伝毒性活性の強さは、変異・がん原性を示すヘテロサイクリックアミンのそれらとほぼ同程度であることから、ABAQ もマウスの肝臓などに発がん性を示すことが予想される。今後、ABAQ の動物を用いた長期発がん実験を行うことが重要と考えられる。

ABAQ の生体内生成の有無について解析するために、野生型、I 型及び II 型糖尿病ラット尿中の ABAQ 量を測定した。その結果、ABAQ 量は、野生型よりも糖尿病モデル動物に於いて高値を示すことが分かった。これらのことから、糖尿病患者の生体内でも ABAQ が生成され、肝臓などの組織に変異を誘発する可能性が推測された。今後、ABAQ のヒト発がんへの関与について解析するために、健常人及び糖尿病患者の尿中 ABAQ 量を詳細に解析することが重要と思われる。

がんの発症促進に肥満が関与することが報告されている。しかし、そのメカニズムは未だ十分にわかっていない。肥満を呈する生体内では、ROS や LPO の産生が増大していることが知られている。そこで、肥満モデルマウス KK-*Ay* における、ROS および LPO 由来の DNA 付加体(8-oxodG、etheno(ε)- and heptanoneε(Hε)deoxyribonucleosides)を、LC/MS/MS を用いて解析した。その結果、20 週齢マウス肝臓における 8-oxodG 量は、正常マウス C57BL に比べ KK-*Ay* で約 3 倍に増加していた。また、εdA、HεdG、HεdA、HεdC 量も、C57BL に比べ KK-*Ay* において 2～3 倍増加していた。これらの結果から、ROS および LPO 由来 DNA 付加体の生成が、肥満関連の発がんに寄与していることが示唆された。今後、腎臓等の他臓器における各種 DNA 付加体量についても解析することが重要と考えられる。

E. 結論

gpt delta マウスに ABAQ を経口投与すると、肝臓における点変異頻度が増加し、G→A 及び G→T 等の点突然変異が誘発されることが分かった。又、ABAQ 投与により肝臓における欠失変異頻度も、3 倍以上上昇することが分かった。更に ABAQ はラットの尿中から検出され、その値は野生型よりも糖尿病モデル動物に於いて高値を示すことが分かった。これらの事から、糖尿病患者の生体内でも ABAQ が生成され、肝臓等の組織に変異を誘発する可能性が推測された。

肥満モデルマウス KK-*Ay* における、ROS および LPO 由来の DNA 付加体(8-oxodG、etheno(ε)- and

heptanoneε(Hε)deoxyribonucleosides)を、LC/MS/MS を用いて解析した。その結果、20 週齢マウス肝臓における 8-oxodG 量は、正常マウス C57BL に比べ KK-A^y で約 3 倍に増加していた。また、εdA、HεdG、HεdA、HεdC 量も、C57BL に比べ KK-A^y において 2～3 倍増加していた。これらの結果から、ROS および LPO 由来 DNA 付加体の生成が、肥満関連の発がんに寄与していることが示唆された。

糖尿病や肥満は、近年、アジア諸国においても急増しており、これら疾病の予防対策は重要な課題となっている。ABAQ 及び酸化損傷に関連する DNA 付加体に関する本研究成果は、糖尿病や肥満とヒト発がんとの関連性を解明する上に有用になると考えられる。

E. 健康危険情報

特になし

F. 研究発表

1. 論文発表

1. Kawanishi M, Ogo S, Ikemoto M, Totsuka Y, Ishino K, Wakabayashi K, Yagi T. Genotoxicity and reactive oxygen species production induced by magnetite nanoparticles in mammalian cells. J Toxicol Sci (2013), in press.
2. Ishikawa H, Wakabayashi K, Suzuki S, Mutoh M, Hirata K, Nakamura T, Takeyama I, Kawano A, Gondo N, Abe T, Tokudome S, Goto C, Matsuura N, Sakai T. Preventive effects of low-dose aspirin on colorectal adenoma growth in patients with familial adenomatous polyposis: Double-blind, randomized clinical trial. Cancer Med (2013), 2:50-56.
3. Matsubara S, Takasu S, Tsukamoto T, Mutoh M, Masuda S, Sugimura T, Wakabayashi K, Totsuka Y. Induction of glandular stomach cancers in *Helicobacter pylori*-infected Mongolian Gerbils by 1-nitrosoindole-3-acetonitrile. Int J Cancer (2012), 130:259-266.
4. Kato T, Totsuka Y, Ishino K, Matsumoto Y, Tada Y, Nakae D, Goto S, Masuda S, Ogo S, Kawanishi M, Yagi T, Matsuda T, Watanabe M, Wakabayashi K. Genotoxicity of multi-walled carbon nanotubes in both *in vitro* and *in vivo* assay systems. Nanotoxicology (2012), published online.
5. Yoshimoto M, Hayakawa T, Mutoh M, Imai T, Tsuda K, Kimura S, Umeda IO, Fujii H, Wakabayashi K. In Vivo SPECT Imaging with ^{111}In-DOTA-c(RGDfK) to Detect Early Pancreatic Cancer in a Hamster Pancreatic Carcinogenesis Model. J Nucl Med (2012), 53:765-771.
6. Ueno T, Imaida K, Yoshimoto M, Hayakawa T, Takahashi M, Imai T, Yanaka A, Tsuta K, Komiya M, Wakabayashi K, Mutoh M. Non-invasive X-ray micro-computed tomography evaluation of indomethacin on urethane-induced

lung carcinogenesis in mice. Anticancer Res (2012), 32:4773-4780.

7. Saika K, Sobue T, Nakamura M, Oshima A, Wakabayashi K, Hamajima N, Mochizuki Y, Yamaguchi R, Tajima K. Smoking prevalence and beliefs on smoking cessation among members of the Japanese Cancer Association in 2006 and 2010. Cancer Sci (2012), 103:1595-1599.
8. Ueno T, Teraoka N, Takasu S, Nakano K, Takahashi M, Yamamoto M, Fujii G, Komiya M, Yanaka A, Wakabayashi K, Mutoh M. Suppressive effect of pioglitazone, a PPAR gamma ligand, on azoxymethane-induced colon aberrant crypt foci in KK-*Ay* mice. Asian Pac J Cancer Prev (2012), 13:4067-4073.

2.学会発表

1. Wakabayashi K, Prevention of Colorecral Cancer, Tokushima Cancer Meeting, Tokushima, Japan, 2012
2. 高須伸二、武藤倫弘、一二三佳恵、若林敬二、中釜 斉、アンジオテンシンII受容体拮抗薬の Min マウス腸ポリープ生成抑制効果、第19回日本がん予防学会、2012年
3. 三好規之、長澤友樹、田中卓二、若林敬二、大島寛史、肥満モデルマウス KK-Ay における山薬およびジオスゲニンの大腸発がん予防分子機構解析、第 19 回日本がん予防学会、2012年
4. 戸塚ゆ加里、石野孔祐、若林敬二、渡辺徹志、中釜 斉、メイラード反応生成物、アミノベンゾアゼピノキノリノン(ABAQ)の in vivo 変異原性と生体内における生成、第 17 回日本癌学会学術総会、2012年
5. Wakabayashi K, Matsubara S, Takasu S, Tsukamoto T, Mutoh M, Totsuka Y, Induction of glandular stomach cancers in Helicobacter pylori-infected Mongolian gerbils by 1-nitrosoindole-3-acetonitrile , The 3rd .Asian Conference on Environmental Mutagens, Hangzhou, China, 2012
6. Watanabe T, Coulibaly S, Hasei T, Funasaka K, Asakawa D, Sera N, Seiyama T, Kido M, Toriba A, Hayakawa K, Tang N, Zhao L, Chung HY, Watanabe M, Wakabayashi K, Trans-boundary air pollution with genotoxic compounds in East Asia, The 3rd Asian Conference on Environmental Mutagens, Hangzhou, China, 2012
7. Totsuka Y, Ishino K, Wakabayashi K, Watanabe T, Masuda S, Nakagama N, *In vivo* mutagenicity and formation of a Maillard reaction product, aminobenzoazepinoquinolinone derivative (ABAQ), The 3rd Asian Conference on Environmental Mutagens, Hangzhou, China, 2012
8. 山田理史、渡辺徹志、大嶽信弘、斎藤貴江子、栗木清典、中嶌輝子、武藤倫弘、若林敬二、太田ポンカン果皮の安全性の検討、第 17 回日本フードファクター学会（JSoFF）学術集会・第9回日本カテ

キン学会総会 合同大会、 2012 年

9. 池本実穂、川西優喜、戸塚ゆ加里、若林敬二、八木孝司、カオリンの遺伝毒性発現メカニズムの解明、日本環境変異原学会第 41 回大会、2012 年
10. 堺澤 絢、後藤純雄、若林敬二、渡辺徹志、中釜 斉、戸塚ゆ加里、トリプトファンとグルコースのメイラード反応生成物アミノベンゾアゼピノキノリノン誘導体の *in vivo* 変異原性，日本環境変異原学会第 41 回大会、2012 年
11. 藤田浩祐、クゥリバリ スレイマン、高橋亮平、貴志茜衣、坂本みずほ、松井元希、長谷井友尋、池盛文数、盛山哲郎、木戸瑞佳、世良暢之、船坂邦弘、浅川大地、鳥羽 陽、早川和一、唐 寧、趙利霞、鄭海泳、若林敬二、渡部仁成、渡辺徹志、東アジア地域 5 地点における大気粉塵の化学成分及び変異原性の比較，日本環境変異原学会第 41 回大会、2012 年
12. 宇田一成、今西稜太郎、遠藤 治、渡辺徹志、大嶽信弘、斉藤貴江子、若林敬二、太田ポンカン果皮抽出物の抗変異原性、日本環境変異原学会第 41 回大会、2012 年

G. 知的財産権の出願・登録状況

1. 特許取得

特になし

2. 実用新案登録

特になし

3.その他

特になし

別紙４

研究成果の刊行に関する一覧表

書籍

著者氏名	論文タイトル名	書籍全体の編集者名	書　籍　名	出版社名	出版地	出版年	ページ
なし	なし						

雑誌

発表者氏名	論文タイトル名	発表誌名	巻号	ページ	出版年
Lim T-H, Fujikane R, Sano S, Sakagami R, Nakatsu Y, Tsuzuki T, Sekiguchi M, Hidaka M	Activation of AMP-activated protein kinase by MAPO1 and FLCN induces apoptosis triggered by alkylated base mismatch in DNA.	DNA Repair	11	259-266	2012
Ella E, Sato N, Nishizawa D, Kageyama S, Yamada H, Kurabe N, Ishino K, Tao H, Taniokа F, Nozawa A, Renyin C, Shinmura K, Ikeda K, Sugimura H.	Association between dopamine beta hydroxylase rs5320 polymorphism and smoking behaviour in elderly Japanese.	J Hum Genet	57	385-390	2012
Matsuda T, Tao H, Goto M, Yamada H, Suzuki M, Wu Y, Xiao N, He Q, Guo W, Cai Z, Kurabe N, Ishino K, Matsushima Y, Shinmura K, Konno H, Maekawa M, Wang Y, Sugimura H.	Lipid peroxidation-induced DNA adducts in human gastric mucosa.	Carcinogenesis	34	121-127	2013
Matsubara S, Takasu S, Tsukamoto T, Mutoh M, Masuda S, Sugimura T, Wakabayashi K, Totsuka Y	Induction of glandular stomach cancers in *Helicobacter pylori*-infected Mongolian Gerbils by 1-nitrosoindole-3-acetonitrile	Int J Cancer	130	259-266	2012

DNA Repair 11 (2012) 259–266

Contents lists available at SciVerse ScienceDirect

DNA Repair

journal homepage: www.elsevier.com/locate/dnarepair

Activation of AMP-activated protein kinase by MAPO1 and FLCN induces apoptosis triggered by alkylated base mismatch in DNA

Teik How Lim[a], Ryosuke Fujikane[b], Shiori Sano[b,c], Ryuji Sakagami[c], Yoshimichi Nakatsu[a], Teruhisa Tsuzuki[a], Mutsuo Sekiguchi[d], Masumi Hidaka[b,*]

[a] Department of Medical Biophysics and Radiation Biology, Faculty of Medical Sciences, Kyushu University, Fukuoka 812-8582, Japan
[b] Department of Physiological Science and Molecular Biology, Fukuoka Dental College, Fukuoka 814-0193, Japan
[c] Department of Odontology, Fukuoka Dental College, Fukuoka 814-0193, Japan
[d] Frontier Research Center, Fukuoka Dental College, Fukuoka 814-0193, Japan

ARTICLE INFO

Article history:
Received 31 August 2011
Received in revised form 9 November 2011
Accepted 28 November 2011
Available online 29 December 2011

Keywords:
AMPK
Apoptosis
Folliculin/BHD
MAPO1/FNIP2/FNIPL
O^6-methylguanine

ABSTRACT

O^6-Methylguanine produced in DNA by the action of simple alkylating agents, such as *N*-methyl-*N*-nitrosourea (MNU), causes base-mispairing during DNA replication, thus leading to mutations and cancer. To prevent such outcomes, the cells carrying O^6-methylguanine undergo apoptosis in a mismatch repair protein-dependent manner. We previously identified MAPO1 as one of the components required for the induction of apoptosis triggered by O^6-methylguanine. MAPO1, also known as FNIP2 and FNIPL, forms a complex with AMP-activated protein kinase (AMPK) and folliculin (FLCN), which is encoded by the *BHD* tumor suppressor gene. We describe here the involvement of the AMPK–MAPO1–FLCN complex in the signaling pathway of apoptosis induced by O^6-methylguanine. By the introduction of siRNAs specific for these genes, the transition of cells to a population with sub-G_1 DNA content following MNU treatment was significantly suppressed. After MNU exposure, phosphorylation of AMPKα occurred in an MLH1-dependent manner, and this activation of AMPK was not observed in cells in which the expression of either the *Mapo1* or the *Flcn* gene was downregulated. When cells were treated with AICA-ribose (AICAR), a specific activator of AMPK, activation of AMPK was also observed in a MAPO1- and FLCN-dependent manner, thus leading to cell death which was accompanied by the depolarization of the mitochondrial membrane, a hallmark of the apoptosis induction. It is therefore likely that MAPO1, in its association with FLCN, may regulate the activation of AMPK to control the induction of apoptosis triggered by O^6-methylguanine.

1. Introduction

Most of the DNA lesions produced by internal and external agents can be removed by cellular DNA repair enzymes, while cells with un-repaired lesions are eliminated by apoptosis. The biological significance of these two mechanisms is clearly shown when organisms lacking one or both of these cellular functions are exposed to simple alkylating agents, such as *N*-methyl-*N*-nitrosourea (MNU) and *N*-methyl-*N'*-nitro-*N*-nitrosoguanidine (MNNG), which alkylate purine and pyrimidine bases in DNA [1]. Among the various modified bases thus produced, O^6-methylguanine is of particular importance since this modified base can pair with thymine as well as cytosine during DNA replication, leading to induction of mutation and cancer [2,3]. Organisms possess a specific DNA repair enzyme, O^6-methylguanine–DNA methyltransferase (MGMT), which transfers a methyl-group from O^6-methylguanine in DNA onto the enzyme molecule, thereby repairing the DNA lesion in a single step reaction [4,5]. When the modified base is not repaired, an O^6-methylguanine–thymine pair is formed through DNA replication and this mismatch can be recognized by a mismatch repair protein complex, composed of MSH2, MSH6, MLH1 and PMS2, which induces apoptosis to exclude cells carrying the mutation-evoking DNA lesions [6–8]. It is noteworthy that *Mgmt*$^{-/-}$ mice, which lack the DNA repair enzyme specific for O^6-methylguanine, are hypersensitive to both the killing and to the tumorigenic action of alkylating chemicals [9–12] and these dual effects can be dissociated by the introduction of an additional defect in mismatch repair genes. Mice with mutations in both alleles of the *Mgmt* and the *Mlh1* genes, the latter encoding a protein involved in the recognition of mismatched base, are as resistant to MNU as are wild-type mice in terms of survival, but are much more susceptible to MNU-induced tumorigenesis than wild-type mice

* Corresponding author at: Department of Physiological Science and Molecular Biology, Fukuoka Dental College, 2-15-1 Tamura, Sawara-ku, Fukuoka 814-0193, Japan. Tel.: +81 92 801 0411x310; fax: +81 92 801 0685.
E-mail address: hidaka@college.fdcnet.ac.jp (M. Hidaka).

1568-7864/$ – see front matter © 2011 Elsevier B.V. All rights reserved.
doi:10.1016/j.dnarep.2011.11.006

[13]. Consistent with these results, *Mgmt*$^{-/-}$ *Mlh1*$^{-/-}$ cells, derived from the gene-targeted mice, are unable to induce apoptosis and show an elevated mutant frequency after MNU treatment [14].

The apoptotic signal initiated through the mismatch recognition complex activates a signaling cascade leading to the cell cycle checkpoints and apoptotic pathways for cell death. Both the release of cytochrome C from the mitochondria as well as the activation of Apaf-1 and caspase-3, hallmarks of the induction of apoptosis, have been demonstrated after the treatment of cells with alkylating agents that produce O^6-methylguanine [14,15]. However, the precise molecular mechanism underlying the signal transduction downstream of mismatch recognition still remains to be determined. To identify the factors involved in the O^6-methylguanine-induced apoptotic process, we screened MNU-resistant clones derived from MNU-sensitive *Mgmt*$^{-/-}$ cells using retrovirus-mediated gene-trap mutagenesis [16]. Mouse-derived KH101 cells, carrying an insertional mutation in one of the alleles of an uncharacterized gene, were unable to induce mitochondrial membrane depolarization as well as caspase-3 activation, after treatment with MNU. In this way, we identified a new gene, designated as *Mapo1* (O^6-methylguanine induced apoptosis 1), which was related to the induction of apoptosis. The mutant frequency of KH101 cells was significantly elevated after the treatment with MNU, thus supporting the notion that the induction of apoptosis, in which the MAPO1 is involved, contributes significantly to the elimination of cells carrying mutation-inducing DNA lesions. A search in the database revealed that the amino acid sequence of the MAPO1 protein is homologous to that of folliculin-interacting protein 1 (FNIP1), which was identified as a protein having the capacity to associate with folliculin [17]. Folliculin is a tumor suppressor protein with unknown biological activity, and is encoded by the *FLCN* gene. Mutations in the *FLCN* gene have been found in patients with Birt-Hogg-Dubé (BHD) syndrome [18,19], which is characterized by the development of hair follicle hamartomas, lung cysts, and an increased risk for renal neoplasia [20–22]. Identification of another folliculin-interacting protein, displaying a similarity in its amino acid sequence to that of FNIP1, was reported by two groups of researchers and the gene responsible was named *FNIP2* and *FNIPL*, respectively [23,24]. The *FNIP2/FNIPL* gene turned out to be the same gene as the human homolog of *Mapo1*. It was also reported that FNIP2/FNIPL, as well as FNIP1, could bind to 5′-AMP-activated protein kinase (AMPK), composed of AMPKα, β and γ subunits, which is an important energy sensor in cells that negatively regulates cell growth and proliferation [25,26].

We report here that a complex composed of MAPO1, FLCN and AMPK is involved in the induction of apoptosis triggered by O^6-methylguanine–thymine mispair. Evidence is presented which shows that during the course of apoptosis induction, the phosphorylation of AMPKα occurs in a MAPO1- and FLCN-dependent manner.

2. Materials and methods

2.1. Cell lines and cell culture

The YT102 (*Mgmt*$^{-/-}$ *Mlh1*$^{+/+}$), YT103 (*Mgmt*$^{-/-}$ *Mlh1*$^{-/-}$) and KH101 (*Mgmt*$^{-/-}$ *Mapo1*$^{+/-}$) cell lines were established as described previously [14,16]. The cells were cultivated in Dulbecco's modified Eagle's medium (D-MEM) supplemented with 10% fetal bovine serum (FBS) at 37 °C in 5% CO_2.

2.2. Chemicals

N-Methyl-*N*-nitrosourea (MNU) was obtained from Sigma. Compound C and AICA-Ribose were purchased from Calbiochem.

2.3. Immunoprecipitation and immunoblotting

To prepare cells expressing Flag-tagged MAPO1 or HA-tagged FLCN, a pIRES-puro3 vector (Clontech) containing mouse-derived *Mapo1* cDNA tagged with Flag epitope at the carboxy terminal end or a pIRES-puro2 (Clontech) vector carrying mouse-derived *Flcn* cDNA tagged with the HA epitope at the amino terminal end was introduced into YT102 cells using Lipofectamine 2000 (Invitrogen) according to the manufacturer's protocol. For the immunoprecipitation, the cells were lysed with NETN buffer (50 mM Tris/HCl (pH 8.0), 150 mM NaCl, 0.2% NP-40, 1 mM EDTA) containing protease inhibitors (Roche). To precipitate the Flag-tagged MAPO1, 10 μl of anti-FLAG M2-agarose (Sigma) were added to the extract, and incubated for 4 h at 4 °C. Alternatively, 10 μl of anti-HA (HA-7)-agarose (Sigma) were added to precipitate the HA-tagged FLCN, and the mixture was incubated overnight at 4 °C. After extensive washing of the beads with NETN buffer, the proteins bound to the beads were eluted in 40 μl of 2× SDS-PAGE sample buffer (120 mM Tris/HCl (pH 6.8), 4% SDS, 20% glycerol, 200 mM DTT, 0.002% bromophenol blue).

For the immunoblotting analyses, immunoprecipitated materials or whole cell extracts prepared by the lysis of cells with 2× SDS-PAGE sample buffer were subjected to SDS-PAGE and electroblotted onto a PVDF membrane (Bio-Rad). Detection was performed using an ECL Plus or Advance Western blotting detection kit (GE Healthcare). The primary antibodies used were: anti-FLAG M2 (Sigma), anti-HA HA-7 (Sigma), anti-FLCN (Protein Tech Group, Inc.), anti-AMPKα (Cell signaling), anti-β-actin (Sigma), and anti-phospho-AMPKα (Thr172) (Cell signaling). Anti-mouse IgG and anti-rabbit IgG conjugated to horseradish peroxidase (GE Healthcare) were used as the secondary antibodies.

2.4. siRNA transfection

Stealth RNAi for the *Mapo1* gene (siMapo1), 5′-CAGAAAGCAGAGGAUGUUCCUAUUA-3′, *Flcn* gene (siFlcn#1), 5′-UUAUUCAGGAUAGUGGGCCCAACUC-3′, (siFlcn#2), 5′-UGGUGACUGACGUACUUAAUAGAGG-3′, and *Ampkα* gene (siAmpkα#1), 5′-UAUCUUAGCGUUCAUCUGGGCAUCC-3′, (siAmpkα#2), 5′-AAGAUGAUAAGCCACUGCAAGCUGG-3′ were purchased from Invitrogen. After culturing 1×10^5 cells in a 6-well plate for one day, the cells were transfected with 20 nM siRNA, using the Lipofectamine RNAiMAX reagent (Invitrogen) according to the manufacturer's protocol. For the control transfection, Stealth RNAi Negative Control Medium GC Duplex (Invitrogen) was used.

2.5. Flow cytometric analysis

For the sub-G_1 population assay, cells were washed with PBS and suspended in 400 μl of PBS containing 0.1% Triton X-100, 25 μg/ml of propidium iodide and 0.1 mg/ml of RNase A. The samples were analyzed using a FACS Calibur flow cytometer (Becton Dickinson), with 10,000 events per determination.

For the mitochondrial membrane depolarization assay, cells were treated with the MitoProbeTM DiOC2(3) Assay Kit (Invitrogen), according to the manufacturer's protocol, and then subjected to analysis using a FACS Calibur flow cytometer.

2.6. Trypan blue exclusion assay

The viability of YT102, KH101 and siRNA-transfected YT102 cells was assayed, based on their trypan blue exclusion. The cells treated with AICA-Ribose were collected 48 h after the drug treatment and were stained with 0.2% trypan blue. The percentage of dead cells was determined as the percentage of trypan blue staining-positive cells. At least 500 cells were counted per experiment.

2.7. Statistics

All *P*-values were generated using two-tailed Student's *t*-tests.

3. Results

3.1. Interaction of MAPO1 with FLCN and AMPK

To confirm that MAPO1 protein interacts with FLCN and AMPK, a co-immunoprecipitation experiment was performed. Whole cell extracts were prepared from mouse YT102 (*Mgmt*$^{-/-}$) cells expressing Flag-tagged MAPO1, and were subjected to immunoprecipitation using an anti-Flag antibody conjugated to agarose beads. The results are shown in Fig. 1A. With whole cell extracts, almost the same intensity of bands for FLCN and AMPKα were detected in both control and Flag-MAPO1-transfected cells. When the materials were immunoprecipitated with the anti-Flag antibody, co-precipitated FLCN and AMPKα were clearly detected, concomitant with the effective precipitation of Flag-MAPO1, whereas no such bands were seen in a sample precipitated from cells treated with the control vector alone.

To evaluate the interaction of FLCN with MAPO1 and AMPK in a reciprocal manner, whole cell extracts prepared from YT102 cells expressing FLAG-tagged MAPO1, with or without HA-tagged FLCN, were applied for immunoprecipitation using an anti-HA antibody (Fig. 1B). When the HA-tagged FLCN was precipitated, as indicated by doublet bands by the immunoblotting analysis, the Flag-tagged MAPO1 and AMPKα were co-precipitated. It is evident, therefore, that MAPO1 interacts with FLCN and AMPK in mouse cells.

3.2. Suppression of the induction of apoptosis in Flcn- and Ampkα-knockdown cells

Since MAPO1 has been identified as an apoptosis-inducing protein, it is plausible that the MAPO1-bound proteins, FLCN and AMPK, might also be involved in apoptosis induction. To examine the possible roles of these proteins, siRNAs specific for the *Flcn* or *Ampkα* genes were introduced into YT102 (*Mgmt*$^{-/-}$) cells. As shown in Fig. 2A and B, two independent siRNAs (siFlcn#1 and #2, and siAmpkα#1 and #2), designed at different sequences of each gene, effectively suppressed the expression of the genes when measured at 48 h after their introduction. The expression level of the *Mapo1* gene in siMapo1-treated cells also decreased to 43% of that in cells that were treated with the control RNA, siCont, as measured by quantitative real time PCR [16]. To monitor the appearance of cells with sub-G_1 DNA content, cells were treated with or without 0.4 mM MNU for 1 h and subjected to a flow cytometric analysis 72 h later. After treatment with MNU, the sub-G_1 cell population increased to more than 20% in the siCont-treated cells (Fig. 2C). Under the same conditions, the degrees of the increases in the cells treated with siRNAs against the *Flcn*, *Ampkα* and *Mapo1* genes were significantly suppressed. These results favor the notion that FLCN and AMPKα, as well as MAPO1, are involved in MNU-induced apoptosis through protein interactions.

3.3. Suppression of the induction of apoptosis by an AMPK inhibitor

The effects of *Ampkα* knockdown on the MNU-induced apoptosis were further examined at multiple time points. The YT102 cells transfected with siCont or siAmpkα#2 were exposed to 0.4 mM MNU for 1 h and then subjected to a flow cytmetric analysis. As shown in Fig. 3A, the sub-G_1 cell population increased gradually, with similar kinetics in cells transfected with either type of siRNA, but the degree of the increase in cells transfected with siAmpkα was significantly lower than that of siCont-transfected cells.

To obtain further evidence supporting the involvement of AMPK in MNU-induced apoptosis, compound C, a specific inhibitor of AMPK, was used to downregulate the function of AMPK. YT102 cells were exposed to 0.4 mM MNU for 1 h, followed by incubation with or without 2 μM of compound C for 72 h, and then cells were subjected to a flow cytometric analysis. As shown in Fig. 3B, the sub-G_1 cell population in compound C-treated cells after MNU treatment significantly decreased in comparison to those not treated with the inhibitor. The inhibitory effects of compound C on AMPK activity were assessed by immunoblotting using an antibody that specifically recognizes a phosphorylated form of AMPKα, since AMPK is activated when the catalytic subunit of AMPKα becomes phosphorylated [27–29]. As shown in Fig. 3C, AMPK appeared to be activated after MNU treatment, while such activation was significantly suppressed by the exposure of cells to compound C. These findings are consistent with the notion that AMPK plays an important role in the induction of apoptosis triggered by MNU.

3.4. MAPO1- and FLCN-dependent activation of AMPK during the induction of apoptosis

To further examine if AMPKα is phosphorylated during the induction of apoptosis, YT102 cells were treated with 1 mM MNU and then collected at 0, 24, 48 and 72 h after treatment. Under these conditions, apoptosis was effectively induced, as was evident by the detection of the mitochondrial membrane depolarization and the caspase-3 activity [16]. The whole cell extracts were prepared, and the phosphorylation levels of AMPKα were assessed by

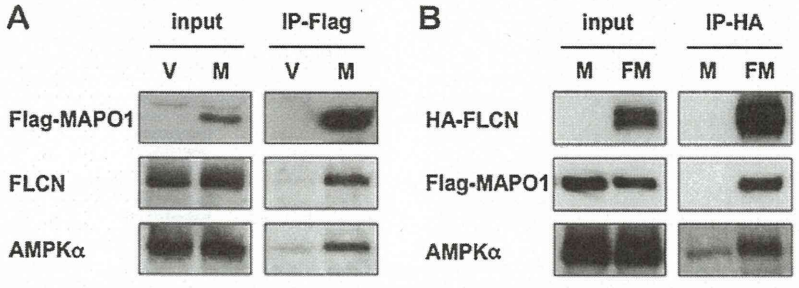

Fig. 1. The association of MAPO1, FLCN and AMPKα proteins. (A) The interaction of MAPO1 with FLCN and AMPKα. YT102 cells were transfected with the pIRES-puro3 vector (termed as V) or pIRES-puro3 containing Flag-tagged *Mapo1* cDNA (termed as M) and harvested after incubation for 24 h. Whole cell extracts (input) were used for immunoprecipitation using anti-Flag M2 antibody beads (IP-Flag). The materials were subjected to SDS-PAGE, transferred to a membrane and immunoblotted using antibodies that recognize the Flag-tag, FLCN and AMPKα. (B) The interaction of FLCN with MAPO1 and AMPKα. YT102 cells were transfected with either pIRES-puro3 containing Flag-tagged *Mapo1* cDNA (termed as M) or pIRE-puro2 carrying HA-tagged *Flcn* cDNA and pIRES-puro3 containing Flag-tagged *Mapo1* cDNA (termed as FM) and were harvested 24 h later. Following immunoprecipitation using anti-HA HA7 antibody beads (IP-HA), an immunoblotting analysis was performed as described in (A) with anti-HA, anti-Flag and anti-AMPKα antibodies.

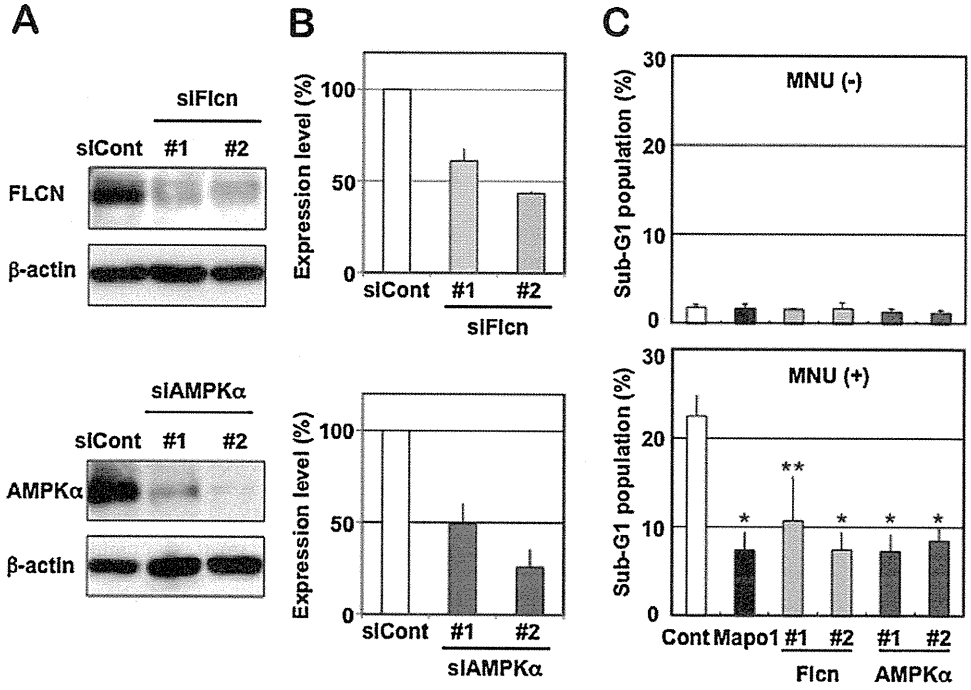

Fig. 2. The suppression of apoptosis by siRNAs targeting the three types of genes. (A) The expression levels of FLCN and AMPKα in cells treated with siRNAs. The whole extracts of YT102 cells transfected with control and two independent siRNAs specific for the corresponding genes were used for the immunoblotting analysis with antibodies specific for FLCN, AMPKα and β-actin (loading control). (B) The relative expression levels of FLCN and AMPKα in the cells treated with siRNAs, as measured by an immunoblotting analysis in (A). (C) The sub-G_1 population of cells transfected with control, *Mapo1*-, *Flcn*- or *Ampkα*-siRNA after MNU treatment. Two days after transfection with siRNA, YT102 cells were treated with or without 0.4 mM MNU for 1 h and then incubated for three days. The cells were harvested and subjected to a flow cytometric analysis. $^{*}P < 0.01$; $^{**}P < 0.05$ when comparing the sub-G_1 populations in the control and gene-specific siRNA-transfected cells.

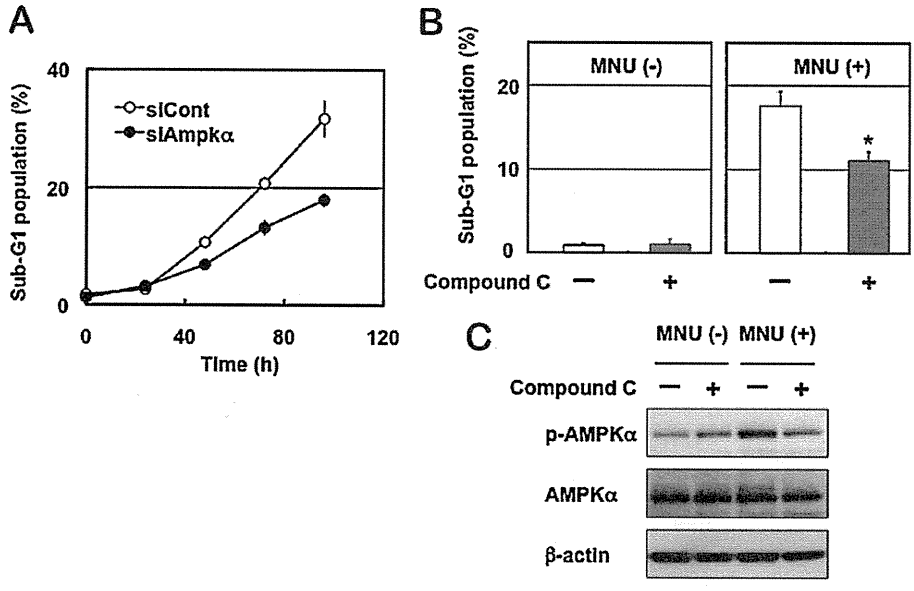

Fig. 3. The involvement of AMPK in MNU-induced apoptosis. (A) The sub-G_1 population of cells transfected with control or *Ampkα* siRNA after MNU treatment. Two days after transfection with siRNA, the YT102 cells were treated with 0.4 mM MNU for 1 h and then harvested at 0, 24, 48, 72 and 96 h after MNU treatment, and subjected to a flow cytometric analysis. The numbers of the cells in the sub-G_1 population were counted and the ratios were plotted. Open circles, siCont-transfected cells; closed circles, siAmpkα-transfected cells. (B) The suppression of apoptosis by an AMPK inhibitor. After treatment with or without 0.4 mM MNU for 1 h, YT102 cells were incubated in medium supplemented with or without 2 μM compound C for three days. The cells were then harvested and subjected to a flow cytometric analysis to monitor the sub-G_1 population of cells. $^{*}P < 0.01$ when comparing the sub-G_1 populations in compound C-untreated and compound C-treated cells after exposure to MNU. (C) The inhibition of the AMPK activity by compound C. The whole cell extracts from the cells harvested at 48 h after MNU treatment were subjected to an immunoblotting analysis using antibodies that recognize phospho-AMPKα (Thr172), AMPKα and β-actin, respectively.

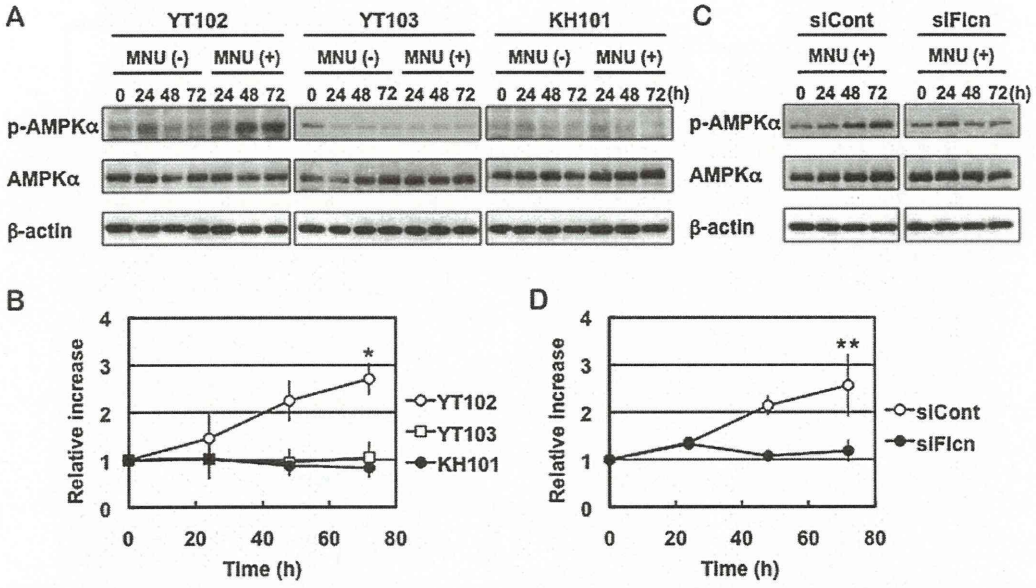

Fig. 4. The activation of AMPK after MNU treatment. (A) The phosphorylation of AMPKα in cells with different genetic backgrounds. Three cell lines, YT102 (*Mgmt*$^{-/-}$), YT103 (*Mgmt*$^{-/-}$ *Mlh1*$^{-/-}$) and KH101 (*Mgmt*$^{-/-}$ *Mapo1*$^{+/-}$), were treated with or without 1 mM MNU for 1 h and then incubated for 0, 24, 48 or 72 h. The whole cell extracts from cells harvested at various times after MNU treatment were subjected to an immunoblotting analysis using antibodies that recognize phospho-AMPKα (Thr172), AMPKα and β-actin, respectively. (B) The relative intensities of the bands for phospho-AMPKα (Thr172) after MNU treatment. Open circles, YT102; open squares, YT103; closed circles, KH101. *$P < 0.01$ when comparing the relative intensities for YT102 cells with those of the YT103 and KH101 cells at 72 h after exposure to MNU. (C) Activation of AMPK in cells transfected with *Flcn*-siRNA. Two days after transfection with control or *Flcn*-siRNA, the YT102 cells were treated with or without 1 mM MNU for 1 h. The analysis was performed as described above. (D) The relative intensities of bands for phospho-AMPKα (Thr172) after MNU treatment. Open circles, siCont-transfected cells; closed circles, siFlcn-transfected cells. **$P < 0.05$ when comparing the relative intensities of the control and *Flcn*-specific siRNA-transfected cells at 72 h after exposure to MNU.

an immunoblotting analysis. As shown in Fig. 4A and B, the levels of phosphorylation of AMPKα increased gradually and reached about 2.7-folds at 72 h after MNU treatment, whereas no such increase was observed in cells not expose to MNU. The amounts of the AMPKα protein were almost constant under these situations. In YT103 (*Mgmt*$^{-/-}$ *Mlh1*$^{-/-}$) cells, which are unable to induce apoptosis due to their lack of the *Mlh1* gene, the increase of phosphorylated forms of AMPKα was hardly detectable, even after MNU treatment. These results indicate that AMPK is activated during the course of the induction of apoptosis, triggered in a mismatch repair protein-dependent manner. To evaluate the effects of *Mapo1* mutation on the activation of AMPK, we used KH101 (*Mgmt*$^{-/-}$ *Mapo1*$^{+/-}$) cells, which carry an insertional mutation in one of the alleles of the *Mapo1* gene and exhibit haploinsufficiency for the induction of apoptosis triggered by MNU treatment [16]. Similar to the results described above, no increase in the band corresponding to phosphorylated AMPKα was detected even after treatment with MNU (Fig. 4A and B). Since MAPO1 interacts with FLCN (Fig. 1), it was supposed that FLCN might also play a role in the activation of AMPK during the course of apoptosis. To examine this possibility, YT102 (*Mgmt*$^{-/-}$) cells were transfected with siRNA targeting the *Flcn* gene (siFlcn#2), and then were exposed to 1 mM MNU for 1 h. The immunoblotting analyses of these samples collected after incubation for 0, 24, 48 and 72 h revealed that phosphorylation of AMPKα, which occurred gradually in siCont-transfected cells, did not take place in the siFlcn-transfected ones (Fig. 4C and D). These results indicate that the activation of AMPK, which occurs during the course of MNU-induced apoptosis, is dependent on the functions of both FLCN and MAPO1.

3.5. Induction of apoptosis through activation of AMPK

To confirm the importance of the activation of AMPK for the induction of apoptosis, AICA-Ribose (AICAR), a specific activator of AMPK, was applied to YT102 cells. After treatment with a low dose (0.2 mM) of AICAR for 48 h, the viabilities of cells were analyzed, based on the trypan blue exclusion assay. As shown in Fig. 5A, there was a significant increase of trypan blue staining-positive cells after treatment with AICAR in the YT102 (*Mgmt*$^{-/-}$ *Mapo1*$^{+/+}$) cells, whereas no such increase was observed in the *Mapo1*-defective KH101 (*Mgmt*$^{-/-}$ *Mapo1*$^{+/-}$) cells even after the same treatment. To determine if the increase in dead cells was related to the induction of apoptosis, the cells were subjected to an assay for mitochondrial membrane depolarization, which is known to occur during the process of apoptosis. The results are shown in Fig. 5B and C. The depolarization of the mitochondrial membrane was induced after treatment with AICAR in YT102 cells, but not in *Mapo1*-defective KH101 cells. The results indicate that the function of MAPO1 is necessary for AICAR-induced apoptosis. An immunoblotting experiment, the results of which are shown in Fig. 5D, revealed that the AICAR-treatment induced phosphorylation of AMPKα to the similar level to that when treated with MNU, however, such an induction did not occur in the *Mapo1*-defective KH101 cells. These results suggest that the activation of AMPK is important for the induction of apoptosis, and that a normal level of MAPO1 is necessary for the activation of AMPK.

We next examined if FLCN, which interacts with MAPO1, is also required for the AICAR-induced cell death. For this study, we applied AICAR to YT102 cells whose FLCN function was knocked down by siRNA (siFlcn#2). As shown in Fig. 6A–C, the degree of AICAR-induced cell death, which was accompanied by the depolarization of the mitochondrial membrane, was significantly lower in siFlcn-transfected cells as compared to that in siCont-transfected ones. Furthermore, the AICAR-induced AMPKα phosphorylation was almost completely blocked in siFlcn-transfected cells (Fig. 6D). Therefore, these results suggest that FLCN is required for AMPK activation, as well as the cell death induced by the treatment with AICAR.

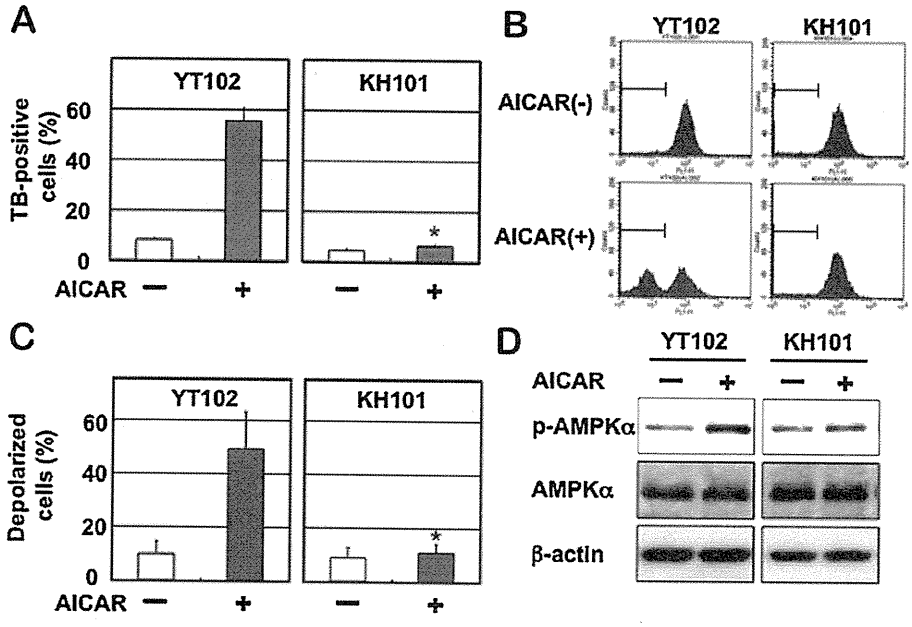

Fig. 5. MAPO1-dependent cell death induced by an AMPK activator. *Mapo1*-proficient YT102 and *Mapo1*-defective KH101 cells were incubated in a medium supplemented with or without 0.2 mM AICAR for two days and then harvested. (A) The viabilities of the cells. The numbers of cells stained with trypan blue (TB) were counted and the ratios are shown. $^*P < 0.01$ when comparing the TB-positive YT102 and KH101 cells after exposure to AICAR. (B) Depolarization of the mitochondrial membrane. The cells were evaluated by a mitochondrial membrane depolarization assay, and representative patterns of the assay are shown. The populations of depolarized cells were gated by bars. (C) The levels of mitochondrial membrane depolarization. The mean values obtained from three independent experiments in (B) and the standard deviations (bars) are presented. $^*P < 0.01$ when comparing the depolarized cells in YT102 and KH101 cells after exposure to AICAR. (D) Activation of AMPK after treatment with AICAR. The whole cell extracts prepared from cells, treated with or without AICAR, were subjected to an immunoblotting analysis using antibodies specific for phospho-AMPKα (Thr172), AMPKα and β-actin, respectively.

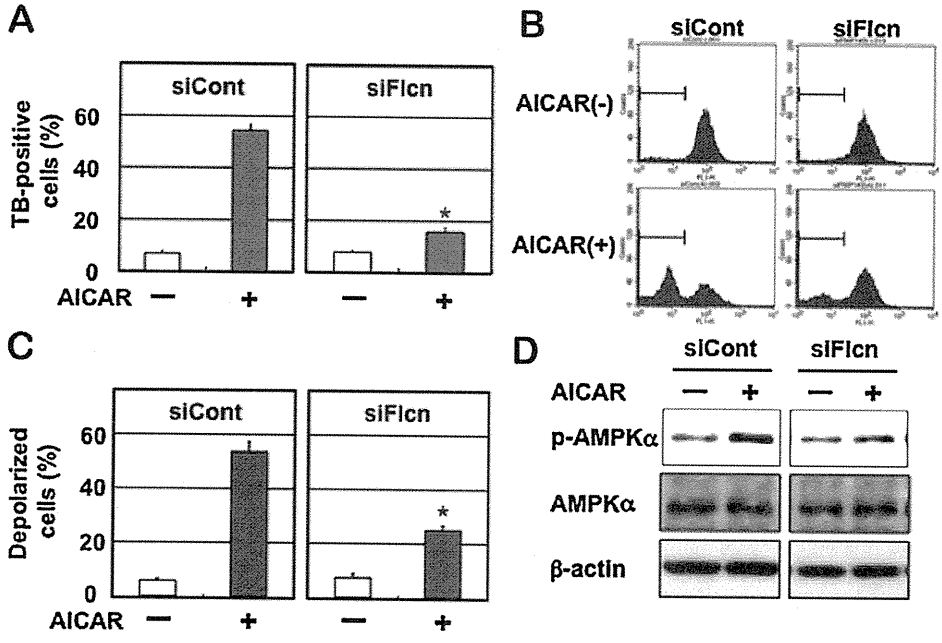

Fig. 6. FLCN-dependent cell death induced by an AMPK activator. YT102 cells transfected with control- or *Flcn*-siRNA were cultured with or without 0.2 mM AICAR for two days and then harvested. (A) The viabilities of the cells. The numbers of cells stained with trypan blue (TB) were counted and the ratios are shown. $^*P < 0.01$ when comparing the TB-positive siCont-transfected and siFlcn-transfected cells after exposure to AICAR. (B) Depolarization of the mitochondrial membrane. The cells were evaluated by a mitochondrial membrane depolarization assay, and representative patterns of the assay are shown. The populations of depolarized cells were gated by bars. (C) The levels of mitochondrial membrane depolarization. The mean values obtained from three independent experiments in (B) and the standard deviations (bars) are presented. $^*P < 0.01$ when comparing the depolarized cells in siCont-transfected and siFlcn-transfected cells after exposure to AICAR. (D) Activation of AMPK after treatment with AICAR. The whole cell extracts prepared from AICAR-treated or -untreated cells, were subjected to an immunoblotting analysis using antibodies specific for phospho-AMPKα (Thr172), AMPKα and β-actin, respectively.

4. Discussion

MAPO1 was identified as one of the protein elements functioning at a certain step following the induction of apoptosis [16]. In *Mapo1*-defective cells, mitochondrial membrane depolarization and caspase-3 activation were not observed even after exposure to MNU, although the cells retain the ability for mismatch repair protein-dependent DNA damage detection and signaling. Subsequent studies have revealed that MAPO1 is identical to FNIP2 and FNIPL, reported by Hasumi et al. [23] and Takagi et al. [24], respectively. This protein is bound to folliculin, encoded by the *FLCN* tumor suppressor gene, and AMP-activated protein kinase (AMPK). To analyze the possible roles of folliculin and AMPK in the induction of apoptosis, we introduced siRNAs specific for the *Flcn* or *Ampkα* gene and then treated the cells with MNU. The flow cytometric analyses performed to measure the sub-G_1 population of cells revealed that folliculin and AMPK, as well as MAPO1, were involved in MNU-induced apoptosis. Taken together, these data suggest that MAPO1 forms a protein complex(es) with folliculin and AMPK, and plays a role in a signal transduction pathway of apoptosis.

It is known that AMPK is one of the signaling kinases that negatively regulates cell growth and proliferation and is phosphorylated itself under conditions of energetic stress [26–29]. Several recent papers have observed the pro-apoptotic potential of activated AMPK [30–33]. In this report, we found a gradual increase in the levels of AMPK phosphorylation in *Mapo1*-proficient cells after MNU treatment, implying a possible involvement of the activation of AMPK in the MNU-induced apoptosis pathway. In *Mapo1*-deficient cells, AMPK activation in this manner was hardly detectable, even after the treatment with MNU. Furthermore, the treatment of cells with AICAR, a specific activator of AMPK, resulted in AMPKα phosphorylation and mitochondrial membrane depolarization in a *Mapo1*-dependent manner. These findings extended onto the case of *Flcn*-knockdown cells. Taken together, it is likely that MAPO1 and FLCN positively regulate the activation of AMPK through their mutual interaction in the apoptotic signaling pathway, triggered by an alkylating agent. MAPO1 and FLCN proteins have been reported to undergo some modifications in cells [17,24]. The treatment with an alkylating agent might affect the modified states of these proteins, and might cause the activation of the protein complex, thus leading to AMPK activation. Another folliculin-interacting protein, FNIP1, which is homologous to MAPO1, is also capable of binding to AMPK [17]. The activation of AMPK might therefore be regulated in more complex ways under the balance of MAPO1 and FNIP1 activities.

Another important problem which remains to be solved is how the AMPK–MAPO1–FLCN complex is activated by the signal delivered from the mismatch repair protein complex, which itself is activated through the interaction with DNA carrying base mismatches. The signal may be delivered by direct physical contact between the two complexes or through the involvement of other protein factors. The protein linking analyses, aided by mass spectrometry, have been performed, but no evidence to show the physical association of the two complexes was obtained (unpublished results). It seems likely, therefore, that some other protein factor(s) might be involved in the signal transduction process. To identify such factors, it would be relevant to extend this approach using retrovirus-mediated gene-trap mutagenesis studies.

Germline mutations in the *FLCN* gene have been identified in patients with Birt-Hogg-Dubé (BHD) syndrome, which is an autosomal dominant disorder characterized by hamartomas of skin follicles, spontaneous pneumothorax, and renal tumors [20–22]. Furthermore, *BHD* heterozygous knockout mice were revealed to develop kidney cysts and tumors as they aged, while *BHD* homozygous null mice displayed early embryonic lethality [34,35]. The recent findings, including this report, strongly suggest that folliculin has physical and/or functional interactions with the AMPK-mTOR signaling pathway [17,34,36]. Mutations in several other tumor suppressor genes, such as *LKB1*, *TSC1* and *TSC2* [29,37], have also been shown to lead to dysregulation of AMPK-mTOR signaling and to the development of other hamartomatous syndromes. Our present findings that folliculin is involved in the induction of apoptosis might shed some light on the physiological roles of *BHD/FLCN* and other related tumor suppressor genes. We are currently establishing *Mapo1* knockout mice to analyze the possible roles of the gene in the suppression of tumor predisposition resulting from environmental stresses.

Conflict of interest statement

The authors declare that there are no conflicts of interests.

Acknowledgments

We thank Drs. H. Hayakawa and Y. Takagi (Fukuoka Dental College, Japan) for helpful discussion. This work was supported by grants (including a Frontier Research Grant) from the Ministry of Education, Culture, Sports, Science and Technology of Japan, and from the Ministry of Health, Labor and Welfare of Japan.

References

[1] D.T. Beranek, Distribution of methyl and ethyl adducts following alkylation with monofunctional alkylating agents, Mutat. Res. 231 (1990) 11–30.
[2] C. Coulondre, J.H. Miller, Genetic studies of the lac repressor. IV. Mutagenic specificity in the lacI gene of *Escherichia coli*, J. Mol. Biol. 117 (1977) 577–606.
[3] T. Ito, T. Nakamura, H. Maki, M. Sekiguchi, Roles of transcription and repair in alkylation mutagenesis, Mutat. Res. 314 (1994) 273–285.
[4] B. Demple, A. Jacobsson, M. Olsson, P. Robins, T. Lindahl, Repair of alkylated DNA in *Escherichia coli*. Physical properties of O6-methylguanine–DNA methyltransferase, J. Biol. Chem. 257 (1982) 13776–13780.
[5] H. Kawate, K. Ihara, K. Kohda, K. Sakumi, M. Sekiguchi, Mouse methyltransferase for repair of O6-methylguanine and O4-methylthymine in DNA, Carcinogenesis 16 (1995) 1595–1602.
[6] P. Branch, G. Aquilina, M. Bignami, P. Karran, Defective mismatch binding and a mutator phenotype in cells tolerant to DNA damage, Nature 362 (1993) 652–654.
[7] M. Hidaka, Y. Takagi, T.Y. Takano, M. Sekiguchi, PCNA-MutSalpha-mediated binding of MutLalpha to replicative DNA with mismatched bases to induce apoptosis in human cells, Nucleic Acids Res. 33 (2005) 5703–5712.
[8] A. Kat, W.G. Thilly, W.H. Fang, M.J. Longley, G.M. Li, P. Modrich, An alkylation-tolerant, mutator human cell line is deficient in strand-specific mismatch repair, Proc. Natl. Acad. Sci. U.S.A. 90 (1993) 6424–6428.
[9] B.J. Glassner, G. Weeda, J.M. Allan, J.L. Broekhof, N.H. Carls, I. Donker, B.P. Engelward, R.J. Hampson, R. Hersmus, M.J. Hickman, R.B. Roth, H.B. Warren, M.M. Wu, J.H. Hoeijmakers, L.D. Samson, DNA repair methyltransferase (Mgmt) knockout mice are sensitive to the lethal effects of chemotherapeutic alkylating agents, Mutagenesis 14 (1999) 339–347.
[10] K. Sakumi, A. Shiraishi, S. Shimizu, T. Tsuzuki, T. Ishikawa, M. Sekiguchi, Methylnitrosourea-induced tumorigenesis in MGMT gene knockout mice, Cancer Res. 57 (1997) 2415–2418.
[11] A. Shiraishi, K. Sakumi, M. Sekiguchi, Increased susceptibility to chemotherapeutic alkylating agents of mice deficient in DNA repair methyltransferase, Carcinogenesis 21 (2000) 1879–1883.
[12] T. Tsuzuki, K. Sakumi, A. Shiraishi, H. Kawate, H. Igarashi, T. Iwakuma, Y. Tominaga, S. Zhang, S. Shimizu, T. Ishikawa, et al., Targeted disruption of the DNA repair methyltransferase gene renders mice hypersensitive to alkylating agent, Carcinogenesis 17 (1996) 1215–1220.
[13] H. Kawate, K. Sakumi, T. Tsuzuki, Y. Nakatsuru, T. Ishikawa, S. Takahashi, H. Takano, T. Noda, M. Sekiguchi, Separation of killing and tumorigenic effects of an alkylating agent in mice defective in two of the DNA repair genes, Proc. Natl. Acad. Sci. U.S.A. 95 (1998) 5116–5120.
[14] Y. Takagi, M. Takahashi, M. Sanada, R. Ito, M. Yamaizumi, M. Sekiguchi, Roles of MGMT and MLH1 proteins in alkylation-induced apoptosis and mutagenesis, DNA Repair (Amst.) 2 (2003) 1135–1146.
[15] K. Ochs, B. Kaina, Apoptosis induced by DNA damage O6-methylguanine is Bcl-2 and caspase-9/3 regulated and Fas/Caspase-8 independent, Cancer Res. 60 (2000) 5815–5824.
[16] K. Komori, Y. Takagi, M. Sanada, T.H. Lim, Y. Nakatsu, T. Tsuzuki, M. Sekiguchi, M. Hidaka, A novel protein, MAPO1, that functions in apoptosis triggered by O6-methylguanine mispair in DNA, Oncogene 28 (2009) 1142–1150.
[17] M. Baba, S.B. Hong, N. Sharma, M.B. Warren, M.L. Nickerson, A. Iwamatsu, D. Esposito, W.K. Gillette, R.F. Hopkins 3rd, J.L. Hartley, M. Furihata, S. Oishi, W. Zhen, T.R. Burke, W.M. Linehan Jr., L.S. Schmidt, B. Zbar, Folliculin encoded

by the BHD gene interacts with a binding protein, FNIP1, and AMPK and is involved in AMPK and mTOR signaling, Proc. Natl. Acad. Sci. U.S.A. 103 (2006) 15552–15557.
[18] M.L. Nickerson, M.B. Warren, J.R. Toro, V. Matrosova, G. Glenn, M.L. Turner, P. Duray, M. Merino, P. Choyke, C.P. Pavlovich, N. Sharma, M. Walther, D. Munroe, R. Hill, E. Maher, C. Greenberg, M.I. Lerman, W.M. Linehan, B. Zbar, L.S. Schmidt, Mutations in a novel gene lead to kidney tumors, lung wall defects, and benign tumors of the hair follicle in patients with the Birt-Hogg-Dube syndrome, Cancer Cell 2 (2002) 157–164.
[19] C.D. Vocke, Y. Yang, C.P. Pavlovich, L.S. Schmidt, M.L. Nickerson, C.A. Torres-Cabala, M.J. Merino, M.M. Walther, B. Zbar, W.M. Linehan, High frequency of somatic frameshift BHD gene mutations in Birt-Hogg-Dube-associated renal tumors, J. Natl. Cancer Inst. 97 (2005) 931–935.
[20] A.R. Birt, G.R. Hogg, W.J. Dube, Hereditary multiple fibrofolliculomas with trichodiscomas and acrochordons, Arch. Dermatol. 113 (1977) 1674–1677.
[21] J.R. Toro, G. Glenn, P. Duray, T. Darling, G. Weirich, B. Zbar, M. Linehan, M.L. Turner, Birt-Hogg-Dube syndrome: a novel marker of kidney neoplasia, Arch. Dermatol. 135 (1999) 1195–1202.
[22] B. Zbar, W.G. Alvord, G. Glenn, M. Turner, C.P. Pavlovich, L. Schmidt, M. Walther, P. Choyke, G. Weirich, S.M. Hewitt, P. Duray, F. Gabril, C. Greenberg, M.J. Merino, J. Toro, W.M. Linehan, Risk of renal and colonic neoplasms and spontaneous pneumothorax in the Birt-Hogg-Dube syndrome, Cancer Epidemiol. Biomarkers Prev. 11 (2002) 393–400.
[23] H. Hasumi, M. Baba, S.B. Hong, Y. Hasumi, Y. Huang, M. Yao, V.A. Valera, W.M. Linehan, L.S. Schmidt, Identification and characterization of a novel folliculin-interacting protein FNIP2, Gene 415 (2008) 60–67.
[24] Y. Takagi, T. Kobayashi, M. Shiono, L. Wang, X. Piao, G. Sun, D. Zhang, M. Abe, Y. Hagiwara, K. Takahashi, O. Hino, Interaction of folliculin (Birt-Hogg-Dube gene product) with a novel Fnip1-like (FnipL/Fnip2) protein, Oncogene 27 (2008) 5339–5347.
[25] D. Carling, The AMP-activated protein kinase cascade – a unifying system for energy control, Trends Biochem. Sci. 29 (2004) 18–24.
[26] D.G. Hardie, The AMP-activated protein kinase pathway – new players upstream and downstream, J. Cell Sci. 117 (2004) 5479–5487.
[27] S.A. Hawley, M. Davison, A. Woods, S.P. Davies, R.K. Beri, D. Carling, D.G. Hardie, Characterization of the AMP-activated protein kinase from rat liver and identification of threonine 172 as the major site at which it phosphorylates AMP-activated protein kinase, J. Biol. Chem. 271 (1996) 27879–27887.
[28] J.M. Lizcano, O. Goransson, R. Toth, M. Deak, N.A. Morrice, J. Boudeau, S.A. Hawley, L. Udd, T.P. Makela, D.G. Hardie, D.R. Alessi, LKB1 is a master kinase that activates 13 kinases of the AMPK subfamily, including MARK/PAR-1, EMBO J. 23 (2004) 833–843.
[29] R.J. Shaw, M. Kosmatka, N. Bardeesy, R.L. Hurley, L.A. Witters, R.A. DePinho, L.C. Cantley, The tumor suppressor LKB1 kinase directly activates AMP-activated kinase and regulates apoptosis in response to energy stress, Proc. Natl. Acad. Sci. U.S.A. 101 (2004) 3329–3335.
[30] C. Cao, S. Lu, R. Kivlin, B. Wallin, E. Card, A. Bagdasarian, T. Tamakloe, W.M. Chu, K.L. Guan, Y. Wan, AMP-activated protein kinase contributes to UV- and H2O2-induced apoptosis in human skin keratinocytes, J. Biol. Chem. 283 (2008) 28897–28908.
[31] R.G. Jones, D.R. Plas, S. Kubek, M. Buzzai, J. Mu, Y. Xu, M.J. Birnbaum, C.B. Thompson, AMP-activated protein kinase induces a p53-dependent metabolic checkpoint, Mol. Cell 18 (2005) 283–293.
[32] R. Okoshi, T. Ozaki, H. Yamamoto, K. Ando, N. Koida, S. Ono, T. Koda, T. Kamijo, A. Nakagawara, H. Kizaki, Activation of AMP-activated protein kinase induces p53-dependent apoptotic cell death in response to energetic stress, J. Biol. Chem. 283 (2008) 3979–3987.
[33] W.B. Zhang, Z. Wang, F. Shu, Y.H. Jin, H.Y. Liu, Q.J. Wang, Y. Yang, Activation of AMP-activated protein kinase by temozolomide contributes to apoptosis in glioblastoma cells via p53 activation and mTORC1 inhibition, J. Biol. Chem. 285 (2010) 40461–40471.
[34] T.R. Hartman, E. Nicolas, A. Klein-Szanto, T. Al-Saleem, T.P. Cash, M.C. Simon, E.P. Henske, The role of the Birt-Hogg-Dube protein in mTOR activation and renal tumorigenesis, Oncogene 28 (2009) 1594–1604.
[35] Y. Hasumi, M. Baba, R. Ajima, H. Hasumi, V.A. Valera, M.E. Klein, D.C. Haines, M.J. Merino, S.B. Hong, T.P. Yamaguchi, L.S. Schmidt, W.M. Linehan, Homozygous loss of BHD causes early embryonic lethality and kidney tumor development with activation of mTORC1 and mTORC2, Proc. Natl. Acad. Sci. U.S.A. 106 (2009) 18722–18727.
[36] X. Piao, T. Kobayashi, L. Wang, M. Shiono, Y. Takagi, G. Sun, M. Abe, Y. Hagiwara, D. Zhang, K. Okimoto, M. Kouchi, I. Matsumoto, O. Hino, Regulation of folliculin (the BHD gene product) phosphorylation by Tsc2-mTOR pathway, Biochem. Biophys. Res. Commun. 389 (2009) 16–21.
[37] K. Inoki, M.N. Corradetti, K.L. Guan, Dysregulation of the TSC-mTOR pathway in human disease, Nat. Genet. 37 (2005) 19–24.

Journal of Human Genetics (2012) 00, 1–6

www.nature.com/jhg

ORIGINAL ARTICLE

Association between dopamine beta hydroxylase rs5320 polymorphism and smoking behaviour in elderly Japanese

Elakeche Ella[1,2], Naomi Sato[2,3], Daisuke Nishizawa[4], Shinji Kageyama[2], Hidetaka Yamada[1], Nobuya Kurabe[2], Keiko Ishino[2], Hong Tao[2], Fumihiko Tanioka[5], Akiko Nozawa[3], Chen Renyin[2,6], Kazuya Shinmura[2], Kazutaka Ikeda[4] and Haruhiko Sugimura[2]

The dopaminergic brain pathway is involved in many addictive behaviours, hence represents a good candidate in the study of smoking behaviour and nicotine addiction. Dopamine beta hydroxylase (DBH) is an enzyme that catalyses the conversion of dopamine into noradrenaline. This study, the first of its kind, was done to investigate the role of *DBH* rs5320 polymorphism in smoking behaviour of elderly Japanese. This was done by collecting blood samples from 2521 subjects with various smoking habits to genotype the *DBH* rs5320 polymorphism. Participants also had to fill out a questionnaire containing questions regarding their lifestyles. Some of the questions were from the Fagerström Test for Nicotine Dependence (FTND) and the Tobacco Dependence Screener (TDS). It was found that male ever-smokers with AA genotype smoked less cigarettes per day than those with GG and AG genotypes. FTND scores were also lowest in male ever-smokers with AA genotype and in female ever-smokers with AG genotype. There was no correlation detected between the TDS scores and any of the genotypes. This study shows that *DBH* rs5320 polymorphism influences nicotine dependence.
Journal of Human Genetics advance online publication, 19 April 2012; doi:10.1038/jhg.2012.40

Keywords: addiction; dopamine beta hydroxylase (*DBH*); Fagerström Test for Nicotine Dependence (FTND); nicotine dependence; single-nucleotide polymorphism (SNP); smoking behaviour; Tobacco Dependence Screener (TDS)

INTRODUCTION

Dopamine beta hydroxylase (DBH) is an enzyme that catalyses the conversion of dopamine to noradrenaline in sympathetic nerves. DBH is expressed in noradrenaline-containing neurons, occurring in both membrane-bound and soluble forms.[1] Because of this, noradrenaline and DBH are released together during synaptic transmission,[2,3] hence they can be found in cerebrospinal fluid, and plasma or serum. The human gene encoding DBH is located on chromosome 9q34.[4] The *DBH* gene is composed of 12 exons and comprises a sequence of approximately 23 kb.[5] Serum DBH activity of human as well as gorilla have been known to be polymorphic for the last 30 years.[6–9] This inter-individual difference in serum DBH of European population has been stated as being mostly related to a promoter polymorphism at the −1021 promoter region (C to T, rs1611115).[10] Furthermore, there are probably a few pathogenetic germline mutations of *DBH* that explain rare congenital deficiency. The amino-acid substitutions from Asparaginate to Glutaminate at codon 100 in the exon 2 of DBH (300C-A transversion), from Valine to Methionine at codon 87 in the exon 1 of DBG (259 G-A transition) and from Asparaginate to Asparagine at codon 331 in the exon 6 (991 G-A transition) together with splice site mutation (IVS1DS, T-C, +2) are known.[11,12] Clinical phenotypes of these deficiencies are mainly severe orthostatic hypotension and other autonomic nerve symptoms. On the other hand, other polymorphisms also have been investigated in view of a possible modulator of human conditions including psychiatric ones.

In this study, we investigated various aspects of smoking behaviour in relation to single-nucleotide polymorphism in *DBH*. The particular polymorphism investigated was the rs5320, as it was found that the minor allele frequency of this polymorphism existed in substantial number in our Japanese sample. This particular polymorphism has been shown to be associated with Parkinson's disease among North Indians,[13] but our study is the first to investigate its involvement in the role of smoking behaviours.

[1]University of Malta Medical School, Mater Dei Hospital, Tal-Qroqq, Msida MSD, Malta; [2]Department of Tumor Pathology, Hamamatsu University School of Medicine, Hamamatsu, Japan; [3]Department of Clinical Nursing, Hamamatsu University School of Medicine, Hamamatsu, Japan; [4]Research Project for Addictive Substances, Tokyo Metropolitan Institute of Medical Science, Tokyo, Japan; [5]Department of Pathology, Iwata City Hospital, Iwata, Japan and [6]Pathology Department, First Affiliated Hospital of Zhenzhou University, Henan, China
Correspondence: Dr H Sugimura, Department of Tumor Pathology, Hamamatsu University School of Medicine, 1-20-1, Handayama, 431-3192 Hamamatsu, Japan.
E-mail: hsugimur@hama-med.ac.jp
or Dr N Sato, Department of Clinical Nursing, Hamamatsu University School of Medicine, 1-20-1, Handayama, 431-3192 Hamamatsu, Japan.
E-mail: naomi25@hama-med.ac.jp
Received 25 January 2012; revised 6 March 2012; accepted 23 March 2012

MATERIALS AND METHODS

Questionnaire

Blood was collected from 2521 subjects (1616 males and 905 females) between the ages of 60 and 94 years. This was done at the Iwata City Hospital during a 5-year period from 2003 to 2008. The participants involved in this experiment had various smoking habits (1349 male ever-smokers (current-smokers and ex-smokers; 83.5%) and 83 female ever-smokers (9.2%)). To be eligible for this experiment, the participants had to be ambulant and be able to communicate orally. All subjects provided written consent before participating in this study. The overall portraits of subjects have been described previously.[14] The participants were required to fill in a questionnaire leaflet containing various questions about lifestyle, including alcohol consumption, smoking, diet and cancer history. They were assisted in filling out the leaflet by professional interviewers. Some of the questions were from the Fagerström Test for Nicotine Dependence (FTND; a test that yields a continuous measure of nicotine dependence),[15] and Tobacco Dependence Screener (TDS; a screening questionnaire for tobacco/nicotine dependence according to the *International Statistical Classification of Diseases and Related Health Problems* (ICD)-10, *Diagnostic and Statistical Manual of Mental Disorders* (DSM)-III-R and DSM-IV), which consists of 10 questions.[16] The questionnaire also included questions about the numbers of cigarettes smoked per day (CPD), the participants' age when they started smoking, how many times current-smokers had tried to quit smoking and how many times ex-smokers had tried to quit smoking before succeeding.

The study design was approved by the Institutional Review Board of Hamamatsu University School of Medicine.

Genotype analysis

DNA was extracted from the blood samples given by the participants using a QIAamp DNA Blood Maxi kit according to the manufacturers' instructions (Qiagen, Hamburg, Germany). A 50 ng sample of each subjects DNA was amplified by PCR, with the primer set for *DBH* rs5320 polymorphism using the StepOne (Applied BioSystems, Carlsbad, CA, USA). The Assay ID is C_12020332_20. Successful genotyping of *DBH* was performed in 100% of the enrolled subjects. The rate of successful genotyping was almost the same as the other genotype.[17]

Statistical analysis

The genotype of the *DBH* rs5320 polymorphism was tested for Hardy–Weinberg equilibrium using the SPSS statistics software (SPSS Japan, Tokyo, Japan). χ^2 tests of each genotype were performed for smoking status and lung cancer history. The CPD values, FTND scores, TDS scores and trial times for quitting smoking were evaluated according to smoking status and each genotype by the Kruskal–Wallis test or Mann–Whitney *U* test (SPSS Japan).

RESULTS

The age, sex and smoking status of the participants have been reported previously[14] and are shown in Table 1. The age of participants whose DNA could be genotyped ranged from 60 to 94, with the mean age for males being 73.1 years and for females being 73.0 years. Most of the male participants (62%) were ex-smokers, whereas most of the female participants (90.8%) had never smoked. Current-smokers of both sexes had higher TDS than ex-smokers of both sexes. The average CPD for male current-smokers was 16.6 and for female current-smokers 12.2.

Most current-smokers were also current drinkers, and never-smokers of both sexes tended to be never-drinkers ($\chi^2=17.7$, $P=0.001$ for males and $\chi^2=42.1$, $P<0.001$ for females). Table 1 also shows that ex-smokers of both sexes went through more trials to quit smoking than current-smokers.

Table 2 shows that most of the male and female participants had the GG genotype of the *DBH* rs5320 polymorphism ($n=1275$, 78.9% for males and $n=693$, 76.6% for females), followed by the AG genotype and finally the AA phenotype (1.4% of males and 1.3% of

Table 1 Subjects profile

Variables	*Males*	P-*value*	*Females*	P-*value*
Number of subjects	1616		905	
Mean age, years (±s.d.)	73.1 (±6.2)		73.0 (±6.4)	
Age distribution, n (%)				
60–64	81 (5.0)		51 (5.6)	
65–69	426 (26.4)		253 (28.0)	
70–74	456 (28.2)		240 (26.5)	
75–79	418 (25.9)		198 (21.9)	
80–84	170 (10.5)		134 (14.8)	
85–89	51 (3.1)		25 (2.8)	
90–	14 (0.9)		4 (0.4)	
Smoking status, n (%)				
Current-smokers	345 (21.3)		30 (3.3)	
Ex-smokers	1004 (62.1)		53 (5.9)	
Never-smokers	267 (16.5)		822 (90.8)	
Mean age according to smoking status, years (± s.d.)				
Current-smokers	72.1 (±6.0)	0.002[a]	70.8 (±5.0)	0.065[a]
Ex-smokers	73.4 (±6.0)		71.8 (±6.4)	
Never-smokers	73.3 (±7.0)		73.2 (±6.4)	
Mean age at start of smoking, years (± s.d.)				
Ever-smokers	19.6 (±3.5)		33.9 (±12.4)	
Current-smokers	19.9 (±4.3)	0.298[b]	36.1 (±13.1)	0.196[b]
Ex-smokers	19.6 (±3.2)		32.7 (±11.9)	
Mean numbers of CPD (± s.d.)				
Ever-smokers	21.1 (±13.0)		13.3 (±8.1)	
Current-smokers	16.6 (±9.1)	<0.001[b]	12.2 (±6.0)	0.604[b]
Ex-smokers	22.7 (±13.7)		13.9 (±9.0)	
Mean numbers of CPD × years (± s.d.)				
Ever-smokers	854 (±582)		402 (±357)	
Current-smokers	852 (±466)	0.057[b]	428 (±304)	0.257[b]
Ex-smokers	855 (±617)		386 (±386)	
Mean FTND score (± s.d.)				
Ever-smokers	3.58 (±2.20)		2.35 (±2.01)	
Current-smokers	3.61 (±2.08)	0.526[b]	2.17 (±1.76)	0.733[b]
Ex-smokers	3.57 (±2.24)		2.47 (±2.17)	
Mean TDS score (± s.d.)				
Ever-smokers	3.07 (±2.48)		2.87 (±2.47)	
Current-smokers	3.75 (±2.41)	<0.001[b]	3.82 (±2.56)	0.022[b]
Ex-smokers	2.84 (±2.47)		2.43 (±2.33)	
Mean number of trial times for quitting smoking in current-smokers (± s.d.)	1.36 (±1.64)		1.24 (±1.55)	
Mean number of trial times for quitting smoking before succeeding in ex-smokers (± s.d.)	2.10 (±1.54)		1.66 (±1.25)	
Drinking status, n (%)[c]				
Current drinkers	853 (52.9)		178 (19.7)	
Ex-drinkers	319 (19.8)		50 (5.5)	
Never-drinkers	442 (27.4)		676 (74.8)	
Lung cancer history, n (%)				
Yes	47 (2.9)		12 (1.3)	
No	1569 (97.1)		893 (98.7)	

Abbreviations: CPD, cigarettes smoked per day; FTND, Fagerström Test for Nicotine Dependence; TDS, Tobacco Dependence Screener.
Ever-smokers: current-smokers and ex-smokers.
[a]Kruskal–Wallis test comparing three statuses.
[b]Mann–Whitney *U* test comparing current-smokers and ex-smokers.
[c]Information about alcohol drinking status were obtained from 1614 male subjects and 904 female subjects.

Table 2 Subjects distribution according to smoking status, lung cancer history and the rs5320 polymorphism of *DBH*

			Smoking status				*Lung cancer history*		
	Genotype	*Total* n *(%)*	*Current-smokers* n *(%)*	*Ex-smokers* n *(%)*	*Never-smokers* n *(%)*	P-*value*[a]	*Yes* n *(%)*	*No* n *(%)*	P-*value*[b]
Males	GG	1275 (78.9)	277 (80.3)	788 (78.5)	210 (78.7)		41 (87.2)	1234 (78.6)	
	AG	319 (19.7)	65 (18.8)	203 (20.2)	51 (19.1)	0.639	5 (10.6)	314 (20.0)	0.195
	AA	22 (1.4)	3 (0.9)	13 (1.3)	6 (2.2)		1 (2.1)	21 (1.3)	
Females	GG	693 (76.6)	22 (73.3)	41 (77.4)	630 (76.6)		7 (58.3)	686 (76.8)	
	AG	200 (22.1)	7 (23.3)	12 (22.6)	181 (22.0)	0.688	5 (41.7)	195 (21.8)	0.277
	AA	12 (1.3)	1 (3.3)	0 (0)	11 (1.3)		0 (0)	12 (1.3)	

[a]The χ^2 tests were performed based on 3×3 tables.
[b]The χ^2 tests were performed based on 3×2 tables.

Table 3 Subjects distribution according to smoking status and lung cancer history

			Smoking status			
	Lung cancer history	*Total* n *(%)*	*Current-smokers* n *(%)*	*Ex-smokers* n *(%)*	*Never-smokers* n *(%)*	P-*value*[a]
Males	Yes	47 (2.9)	2 (0.6)	44 (4.4)	1 (0.4)	<0.001
	No	1569 (97.1)	343 (99.4)	960 (95.6)	266 (99.6)	
Females	Yes	12 (1.3)	0 (0)	1 (1.9)	11 (1.3)	0.689
	No	893 (98.7)	30 (100)	52 (98.1)	811 (98.7)	

[a]The χ^2 tests were performed based on 2×3 tables.

females). Although it may be possible that some kind of population bias exist in this rural population, we tested this genotype if it is in accordance with the Hardy–Weinberg equilibrium. Actually the genotype distribution obeyed the Hardy–Weinberg equilibrium ($\chi^2 = 0.179$, $P = 0.914$ for males and $\chi^2 = 0.332$, $P = 0.842$ for females). Smoking status (current-smokers, ex-smokers and never-smokers) was not significantly different between the three genotypes, nor was lung cancer history.

Table 3 shows subjects distribution according to smoking status and lung cancer history. It shows a significant relationship between lung cancer history and ex-smokers in males ($P < 0.001$); however, there was no significant relationship between the *DBH* rs5320 polymorphism and lung cancer history in male ex-smokers. Most cases of lung cancer history occurred in male ex-smokers with GG genotype, but not statistically significant (Table 4).

The *DBH* rs5320 polymorphism was shown to be of significance in both males and females with regard to FTND, and in males only with regard to CPD (Table 5). Males with AA genotype smoked less cigarettes per day, while those with GG and AG smoked similar number of cigarettes per day. Male ever-smokers with AA genotype also had lower FTND scores than those with AG and GG genotypes, while female ever-smokers with AG genotype had the lowest FTND scores.

Table 4 Subjects distribution according to lung cancer history and the rs5320 polymorphism of *DBH* in male ex-smokers

		Lung cancer history		
Genotype	*Total* n *(%)*	*Yes* n *(%)*	*No* n *(%)*	P-*value*[a]
GG	788 (78.5)	38 (86.4)	750 (78.1)	
AG	203 (20.2)	5 (11.4)	198 (20.6)	0.208
AA	13 (1.3)	1 (2.3)	12 (1.3)	

[a]The χ^2 test was performed based on 3×2 table.

DISCUSSION

The dopaminergic brain pathway is one that has been studied extensively in regards to addictive behaviour due to the shared characteristics of drug abuse to elicit the release dopamine. Because of this, genes involved in dopamine metabolism represent good candidates in the study of addictive behaviours, such as smoking.

This study specifically shows a significant correlation between the CPD in males and FTND in males and females and the *DBH* polymorphism. Males with AA genotype tend to be the least dependent on nicotine, having the lowest CPD and FTND scores, while females with AG genotype had the lowest FTND scores.

DBH polymorphisms have been investigated from the standpoint of DBH deficiency, several neurological diseases, from migraine[18] to attention-deficit hyperactivity disorder,[19] hypertension[20] and cocaine dependence.[21] The promoter polymorphism has been reported to be associated with Alzheimer's disease.[22]

Several polymorphisms of *DBH* have been studied in terms of the association of smoking behaviour. Among them the promoter polymorphism −1021C/T (rs1611115) is the most extensively